Molecular Genetics and Metabolism 110 (2013) 352–361

Contents lists available at ScienceDirect

Molecular Genetics and Metabolism

journal homepage: www.elsevier.com/locate/ymgme

Genotype–phenotype spectrum of *PYCR1*-related autosomal recessive cutis laxa

Aikaterini Dimopoulou [a,1], Björn Fischer [a,b,1], Thatjana Gardeitchik [c,1], Phillipe Schröter [a], Hülya Kayserili [d], Claire Schlack [a], Yun Li [e,f,g], Jaime Moritz Brum [h], Ingeborg Barisic [i], Marco Castori [j], Christiane Spaich [k], Elaine Fletcher [l], Zeina Mahayri [m], Meenakshi Bhat [n], Katta M. Girisha [o], Katherine Lachlan [p], Diana Johnson [q], Shubha Phadke [r], Neerja Gupta [s], Martina Simandlova [t], Madhulika Kabra [s], Albert David [u], Leo Nijtmans [c], David Chitayat [v], Beyhan Tuysuz [w], Francesco Brancati [x,y], Stefan Mundlos [a,b,z], Lionel Van Maldergem [aa,2], Eva Morava [c,ab], Bernd Wollnik [e,f,g], Uwe Kornak [a,b,*]

[a] *Institut fuer Medizinische Genetik und Humangenetik, Charité-Universitaetsmedizin Berlin, Augustenburger Platz 1, Berlin, Germany*
[b] *Max-Planck-Institut fuer Molekulare Genetik, FG Development & Disease, Berlin, Germany*
[c] *Department of Pediatrics, Radboud University Nijmegen Medical Centre, Nijmegen, The Netherlands*
[d] *Medical Genetics Department, Istanbul Medical Faculty, Istanbul University, Istanbul, Turkey*
[e] *Institute of Human Genetics, University of Cologne, Cologne, Germany*
[f] *Center for Molecular Medicine Cologne, University of Cologne, Cologne, Germany*
[g] *Cologne Excellence Cluster on Cellular Stress Responses in Aging-Associated Diseases (CECAD), University of Cologne, Cologne, Germany*
[h] *Rede SARAH de Hospitais de Reabilitação, Brasilia, DF, Brazil*
[i] *Children's University Hospital Zagreb, Zagreb, Croatia*
[j] *Department of Molecular Medicine, Medical Genetics, San Camillo-Forlanini Hospital, Sapienza University, Rome, Italy*
[k] *Institut für Klinische Genetik, Olgahospital, Klinikum Stuttgart, Stuttgart, Germany*
[l] *Western General Hospital, Edinburgh, Scotland, UK*
[m] *Cytogenetic Unit, Assad University Hospital, Damascus, Syria*
[n] *Centre for Human Genetics, Biotech Park, Bangalore, India*
[o] *Division of Medical Genetics, Department of Pediatrics, Kasturba Medical College, Manipal University, Manipal, India*
[p] *Wessex Clinical Genetics Service, Princess Anne Hospital, Southampton, UK*
[q] *Clinical Genetics Department, Sheffield Children's NHS Foundation Trust, Sheffield, UK*
[r] *Department of Medical Genetics, Sanjay Gandhi Postgraduate Institute of Medical Sciences, Lucknow, India*
[s] *Department of Pediatrics, All India Institute of Medical Sciences, New Delhi, India*
[t] *Clinical Genetics Unit, Motol Hospital, Charles University, Prague, Czech Republic*
[u] *Unité de Génétique Clinique, CHU, Nantes, France*
[v] *The Prenatal Diagnosis and Medical Genetics Program, Department of Obstetrics and Gynaecology, Mount Sinai Hospital, University of Toronto, Toronto, Ontario, Canada*
[w] *Istanbul University, Cerrahpasa Medical Faculty, Department of Pediatric Genetics, Istanbul, Turkey*
[x] *Department of Medical, Oral and Biotechnological Sciences, Gabriele D'Annunzio University, Chieti, Italy*
[y] *Medical Genetics Unit, Policlinico Tor Vergata University Hospital, Rome, Italy*
[z] *Berlin-Brandenburg Center for Regenerative Therapies, Charité-Universitaetsmedizin Berlin, Germany*
[aa] *Centre de Génétique Humaine, Universite´ de Franche-Comté, Besançon, France*
[ab] *Tulane University Medical Center, Hayward Genetics Center, New Orleans, LA, USA*

ARTICLE INFO

Article history:
Received 16 June 2013
Received in revised form 12 August 2013
Accepted 14 August 2013
Available online 24 August 2013

Keywords:
Autosomal recessive cutis laxa
PYCR1
Proline
Mitochondria
Segmental progeroid disorders

ABSTRACT

Autosomal recessive cutis laxa type 2B (ARCL2B; OMIM # 612940) is a segmental progeroid disorder caused by mutations in *PYCR1* encoding pyrroline-5-carboxylate reductase 1, which is part of the conserved proline *de novo* synthesis pathway. Here we describe 33 patients with *PYCR1*-related *ARCL* from 27 families with initial diagnoses varying between wrinkly skin syndrome, gerodermia osteodysplastica, De Barsy syndrome or more severe progeria syndromes. Given the difficult differential diagnosis of ARCL syndromes we performed a systematic comparison of clinical features of *PYCR1*-related ARCL. Intrauterine growth retardation, a characteristic triangular facial gestalt, psychomotor retardation, and hypotonia were the most relevant distinctive hallmarks of ARCL due to proline *de novo* synthesis defects. Corneal clouding or cataracts, athetoid movements, and finger contractures were rather rare features, but had a high predictive value. In our cohort we identified 20 different *PYCR1* mutations of which seven were novel. Most of the mutations accumulated in exons 4 to 6. Missense alterations of highly conserved residues were most frequent followed by splice site changes and a single nonsense mutation.

* Corresponding author at: Institut fuer Medizinische Genetik und Humangenetik, Charité-Universitaetsmedizin Berlin, Augustenburger Platz 1, Berlin, Germany.
E-mail address: uwe.kornak@charite.de (U. Kornak).
[1] Authors contributed equally.
[2] Coordinator Cutis laxa Debré-type Study Group.

http://dx.doi.org/10.1016/j.ymgme.2013.08.009

Proline
Mitochondria
Segmental progeroid disorders

Analysis of genotype–phenotype correlation revealed that patients with mutations in the first two exons had lower average clinical scores and absent or only mild intellectual disability. Structural analyses predicted interference with PYCR1 multimerization for a subset of missense mutations. These findings have implications for the clinics as well as the pathomechanism of *PYCR1*-related ARCL.

1. Introduction

Although cutis laxa disorders were named after the characteristic skin phenotype present in patients, they are usually multi-systemic disorders involving the skeletal, cardiovascular, pulmonary and central nervous systems, depending on the underlying genetic defect. Cutis laxa can be inherited either in an X-linked, autosomal dominant, or autosomal recessive fashion. In autosomal dominant forms of cutis laxa (ADCL) mutations in genes encoding diverse components of the extracellular matrix are found [1]. Autosomal recessive cutis laxa (ARCL) is more heterogeneous in terms of clinical manifestations and the underlying genetic defect. The disease spectrum can be subdivided into autosomal recessive cutis

Fig. 1. Facial phenotype of patients carrying *PYCR1* mutations. (A) Facial images are arranged according to the ages of the affected individuals, the number of each individual is given in the upper left of each picture. (B) Changes of the facial phenotype in patients 7 and 28, ages given at the lower right. In all patients a triangular face, short nose, long philtrum and large ears are visible. Note the striking variability of the phenotype in the first months of life. While patient 23 had a severe progeroid appearance, patients 20 and 1 were less dysmorphic and patient 2 was stated to have a normal facial appearance. Lax facial skin was pronounced in patients 7 and 17, but less obvious in the other patients. In general skin laxity became less severe with age, which is especially obvious in patient 7. In the older patients the dysmorphism became weaker, but the chin became very prominent resulting in prognathism. Patient 10 was also partially described by Gardeitchik et al. [34].

laxa types I and II. Autosomal recessive cutis laxa type I (ARCL1; OMIM 219100) is mainly characterised by severe systemic involvement including pulmonary emphysema, cardiovascular problems, and gastrointestinal manifestations. It is caused by mutations in Fibulin-5 (*FBLN5*) and EGF-containing fibulin-like extracellular matrix protein 2 gene (*EFEMP2*) (formerly fibulin-4 (*FBLN4*)), which results in a more severe phenotype [2–4]. Another form of ARCL1 is caused by mutations in latent transforming growth factor-beta binding protein-4 (*LTBP4*) [5,6]. The mutations identified in ARCL2 affect intracellular gene products with functions in Golgi apparatus, endosomes, or mitochondria. Gerodermia osteodysplastica (GO; OMIM 231070) resides at the milder end of the ARCL2 phenotypic spectrum. The condition is characterised by lax skin and wrinkles at the dorsa of hands and feet, spontaneous bone fractures due to osteoporosis, jaw hypoplasia and usually normal intellectual development. Hennies and colleagues described disease-causing mutations in *GORAB*, encoding a newly identified golgin and interaction partner of RAB6 [7]. Another form of ARCL, wrinkly skin syndrome/autosomal recessive cutis laxa Debré type (ARCL2A; OMIM 219200), is due to mutations in *ATP6V0A2* [8]. This gene encodes the V-type H^+-ATPase subunit a2, which resides in the Golgi apparatus of skin fibroblasts and plays a role in Golgi membrane trafficking. Clinical hallmarks are generalized cutis laxa, delayed closure of the enlarged anterior fontanel, varying degree of developmental delay, cobblestone-like brain malformations and occasionally a neurodegenerative phenotype with seizures and dementia. On biochemical evaluation a specific combined defect of N- and O-glycosylation of serum proteins (CDG type II) is found in these patients [8–12].

Macrocephaly, alopecia, cutis laxa, and scoliosis syndrome (MACS; OMIM 613075) is caused by mutations in *RIN2*. RIN2 is localized on endosomal vesicles and deficiency of this Rab5 effector protein causes a very rare phenotype with a typical facial coarsening, sagging chin, thick lips, mild alterations in serum protein glycosylation and mental retardation [13,14].

At the most severe end of the ARCL spectrum resides the De Barsy syndrome (DBS; OMIM 219150), which has been also referred to as ARCL type III (ARCL3). The clinical hallmarks are a progeroid appearance with short stature, corneal clouding, hypotonia, a movement disorder and pronounced intellectual disability [15,16]. The aetiology of DBS is not fully understood. Mutations in *ATP6V0A2* were described to cause a DBS-like phenotype in a patient with a severe form of ARCL2A [17]. Recently, mutations in *PYCR1* (ARCL2B; OMIM 612940) encoding the pyrroline-5-carboxylate reductase 1 were identified in patients initially diagnosed with DBS [18]. In addition, *ALDH18A1* (P5CS) mutations also cause a syndrome with severe progeroid and neurocutaneous features highly comparable with ARCL2B and the spectrum of De Barsy-like pathologies [19]. Both PYCR1 and ALDH18A1 are multimeric protein complexes and reside in mitochondria where they are involved in *de novo* proline biosynthesis and NAD(P)H + H^+ consumption, which was postulated to function as a proline cycle transporting redox equivalents into mitochondria [20]. PYCR1 deficient patient fibroblasts show an altered mitochondrial membrane potential (MMP), an increased fragmentation of the mitochondrial network and higher apoptosis rates upon oxidative stress [18]. Structural analysis revealed that the active PYCR1 enzyme has a ring-like shape formed by five homodimers [21]. While the enzymatically active centres lie at the outside of this ring its inside forms a negatively charged channel of unknown function. Homodimers are held together by hydrophobic interactions and hydrogen bonds while dimer–dimer binding is mediated by hydrogen bonds and interaction of proline residues [21].

The current study focuses on the clinical features and the molecular genetic basis of *PYCR1*-related cutis laxa. Here we describe 33 patients carrying *PYCR1* mutations and analyse genotype–phenotype

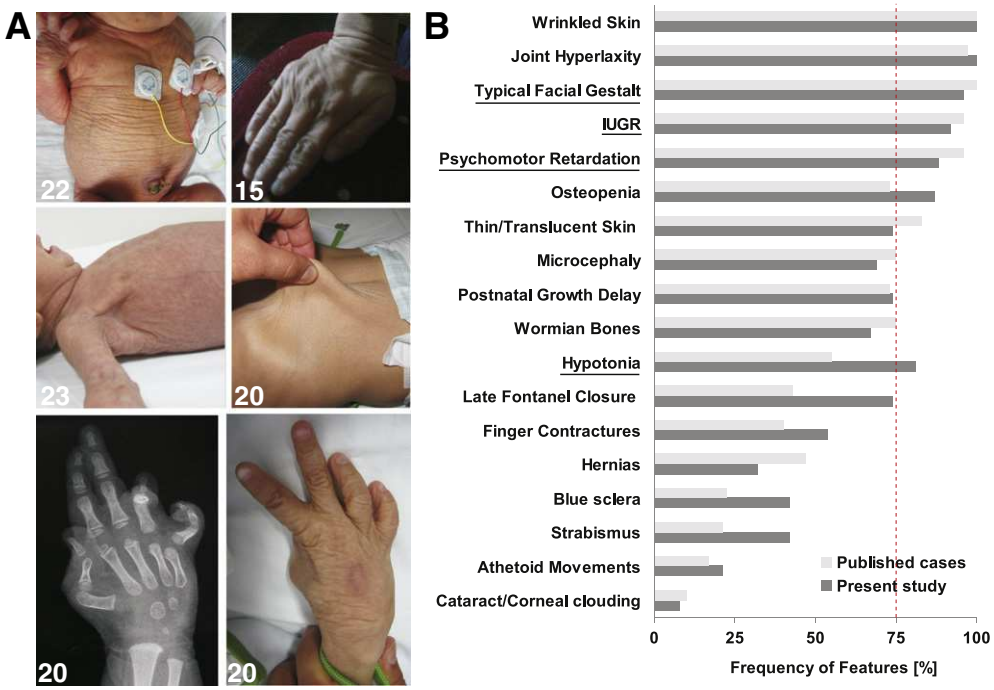

Fig. 2. Further clinical manifestations in *PYCR1*-related CL affected individuals. (A) Clinical features: The number of each individual is given in the lower left of each picture. Severe cutis laxa at abdomen of patient 22. Cutis laxa at the hand of patients 23 and 20. Excess skin in the armpit of patient 23. Loose skin fold of the abdomen of patient 20. Arthrogryposis of the wrist with syn- and clino-dactyly in patient 20. (B) Frequency of clinical features of *PYCR1*-related ARCL patients described in literature and in our 33 patients investigated in this study. The most common features (present in >75% of cases) that allow to distinguish *PYCR1*-related ARCL from the other forms of ARCL types II and III are underlined.

correlation as well as structural aspects of residues affected by missense mutations.

2. Material and methods

2.1. Patients

In this study we evaluated 33 patients with features suggesting ARCL2B, *PYCR1*-related cutis laxa. These criteria included: generalized skin wrinkling, intrauterine growth retardation, a typical facial gestalt, and variable CNS involvement. Peripheral blood was obtained from all patients analysed. Genomic DNA was extracted according to standard procedures. Initial laboratory evaluation included array CGH, karyotype analysis and homozygosity mapping for some cases. Consent for molecular studies was given by all individuals involved in this study or from their legal representatives. The Charité Medical University ethics committee approved the study. The study was performed according to the declaration of Helsinki. Written consent for publication of photographs in Figs. 1 and 2 was given by the patients or their legal representatives.

2.2. Comparison of clinical features

To compare clinical features of individuals with *PYCR1* mutations we determined the presence or absence of each clinical feature. From these values, we calculated the frequency of features. These values were compared to the data analysed previously for 54 individuals from literature with *PYCR1*-related cutis laxa.

2.3. PYCR1 mutation screening

Sequencing of all exons and the flanking intron regions of the *PYCR1* (NM_006907.2) gene was performed as described previously [18] in each tested individual or the parents as obligate heterozygous carriers. All mutations were tested for segregation in the patient's families (if available). Sequencing reaction was performed with the BigDye Terminator cycle sequencing kit (Applied Biosystems, Foster City, CA), and run on an ABI 3730 DNA Analyzer (Applied Biosystems, Foster City, CA). Sequences were evaluated and compared to reference sequences with DNASTAR (DNASTAR Madison, USA). The molecular diagnostic tests were performed in an accredited laboratory (No.: DAP-ML-3869.00, ISO 15189:2003 and ISO/IEC 17025:2005). Functional effects of missense mutations were examined by assessing evolutionary conservation of the affected residues by BLAST alignment and interspecies comparison using MutationTaster and PolyPhen2 and Bioedit [22].

2.4. Phenotype–genotype statistics

Scores for each clinical feature were given according to a scale from 0 = absent to 3 = severe. For hip dislocation, adducted thumb, hernia, and corneal clouding/cataract 1 corresponds to unilateral, mild, 2 to bilateral, mild, and 3 to bilateral, severe. The rating was done by the referring clinicians using a standardized questionnaire. The sum of all individual scores divided by the number of features for which a score was determined gave the average clinical score. Since neurodevelopmental clinical features (psychomotor retardation, dysgenesis/agenesis of corpus callosum, athetoid movements, corneal clouding/cataract) play a greater role for the overall disease severity scores for these features were multiplied by 2. The significance of the correlation between types and position of *PYCR1* mutations and clinical scores were calculated by two-sided, unpaired *t*-test using the Excel (Microsoft, Seattle, USA) software.

2.5. Structural modelling

The 3D structure of PYCR1 was reconstructed by loading the PDB file 2GER containing the published structure [21] into PyMOL1.1 (DeLano Scientific, Palo Alto, CA, USA). Mutated residues were coloured in yellow and the structure surface was inspected.

3. Results

3.1. Clinical findings and comparison with literature

A detailed overview of the clinical features and the corresponding HPO terms in the individual patients is presented in Table 1 [23]. Most newborns, except for patient 2, already presented with a unique facial gestalt, which comprises a typical triangular face due to a hypoplastic viscerocranium (Fig. 1). In some patients a very pronounced progeroid facial appearance was evident at birth (Fig. 1 patients 1 and 23). Although in relation the neurocranium seemed enlarged, microcephaly was noted in 19 patients. Most cases had large, prominent ears and older affected individuals tended to show a prominent chin and prognathism (Fig. 1). All patients presented with lax, wrinkled skin, most prominent on the abdomen, on hand and feet (Fig. 2A). Sagging facial skin was only noted in a subset of patients (Fig. 1). Translucent skin with visible veins was reported in 24 patients (Fig. 2A). Growth parameters were available from 27 patients. In 23 patients the growth restriction was noted prenatally and in 21 it continued postnatally. Progeroid features and growth delay usually got milder during the first years of development. The two affected individuals from family III (4, 5) died in childhood due to a trauma and for unknown reason, respectively. A relation to the genetic disease is unclear.

Central nervous system involvement was described in 28 patients. 27 patients had psychomotor developmental delay and three normal intellectual development. Hypotonia was noted in 25 patients, nine patients showed extrapyramidal symptoms and three patients suffered from epilepsy. A brain MRI was performed in 11 patients. Four patients had corpus callosum dysgenesis and in one patient the cingulate gyrus was also affected. In addition, cranial CT imaging in three individuals showed severe cerebral atrophy and abnormal frontal gyration (segmental pachygyria).

Ophthalmological features were described in 20 patients: 12 patients had strabismus, 13 patients had blue sclera, four had either cataract or corneal clouding and one patient had congenital glaucoma. Adduction of the thumbs was described in 13 patients, however, affected individual 20 additionally showed clino- and syndactyly (Fig. 2A).

In comparison to the clinical features of patients with *PYCR1* mutations reported in the literature (Fig. 2B) we found a significant overlap in the clinical manifestations. Features observed in more than 75% of the cases analysed are thin, wrinkled skin, joint hyperlaxity, typical facial gestalt, intrauterine growth retardation (IUGR), osteopenia, hypotonia and psychomotor retardation (Fig. 2B). While a considerable number of patients showed finger contractures, Wormian bones, blue sclerae and/or strabismus only a minority suffered from corneal clouding or cataract (Fig. 2B).

3.2. PYCR1 mutation screening

We screened all *PYCR1* exons including the alternative additional exon 8 for mutations (Supplementary Fig. 1A). In order to estimate the relevance of transcript B containing this alternative exon transcript-specific qPCR was performed showing a very low expression of this transcript in all cell types tested (Supplementary Fig. 1B). We detected 20 different mutations in 33 patients: one nonsense, five splice site, and 14 missense alterations (Table 2). Seven of these mutations (p.Gly4Val, p.Gly4Asp, c.138 + 2T>C, p.Val117Phe, p.Gly192Val, p.Ala241Asp, p.Ala260Pro) were novel and resided in exons 1, 2, 4, 5, and 6 (Fig. 3A). Five patients were compound heterozygous for a missense and a splice

Table 1
Phenotypic findings and scoring.

Phenotypic findings												
HPO terms			HP:0001511	HP:0001510	HP:0000973	HP:0000963	HP:0001388	HP:0001181	HP:0002827	HP:0100790	HP:0000938	HP:0002645
Family no.	Patient no.	Origin	IUGR	Postnatal growth delay	Lax wrinkled skin	Thin, translucent skin	Joint hyperlaxity	Adducted thumb	Hip dislocation	Hernias	Osteopenia	Wormian bones
I	1	India	2	2	2	2	2	0	1	0	1	n.d.
II	2	India	2	1	1	1	1	0	1	0	0	0
	3	India	n.d.	1	1	0	2	0	1	0	0	0
III	4	Brazil	1	1	1	0	1	1	n.d.	0	n.d.	n.d.
	5	Brazil	1	1	1	0	1	1	n.d.	1	n.d.	n.d.
IV	6	Pakistan	2	0	2	2	1	0	0	0	3	1
V	7	France	2	0	2	0	1	0	0	1	n.d.	n.d.
VI	8	Latvia	1	1	1	1	1	0	0	0	1	n.d.
VII	9	Turkey	1	0	3	2	2	1	1	0	2	1
VIII	10	Iraq	0	1	1	1	1	1	1	0	1	0
IX	11	Czech Rep.	1	1	3	0	n.d.	n.d.	n.d.	n.d.	n.d.	n.d.
X	12	Italy	2	2	2	2	3	0	2	0	n.d.	n.d.
XI	13	Turkey	0	1	1	1	1	0	0	0	n.d.	n.d.
XII	14	Syria	n.d.	3	1	3	0	n.d.	n.d.	1	1	n.d.
	15	Syria	n.d.	n.d.	1	2	n.d.	n.d.	n.d.	1	n.d.	n.d.
	16	Syria	n.d.	n.d.	3	2	n.d.	n.d.	n.d.	1	n.d.	n.d.
XIII	17	India	2	2	3	3	3	2	2	0	n.d.	n.d.
XIV	18	Italy	1	0	1	1	2	0	1	0	2	1
XV	19	India	n.d.	2	1	1	1	2	2	2	1	2
XVI	20	Turkey	3	2	2	2	2	1	0	2	1	0
XVII	21	Turkey	3	0	2	2	2	0	0	0	1	1
XVIII	22	Turkey	1	1	3	3	n.d.	1	1	n.d.	n.d.	n.d.
XIX	23	Turkey	2	1	2	2	1	2	0	0	n.d.	n.d.
	24	Turkey	n.d.	n.d.	1	1	n.d.	n.d.	1	n.d.	n.d.	n.d.
XX	25	Croatia	2	1	2	0	2	2	0	0	2	n.d.
XXI	26	Turkey	1	1	1	1	1	1	0	0	n.d.	n.d.
XXII	27	Germany	2	1	3	1	1	0	2	1	1	n.d.
XXIII	28	France	3	1	2	0	1	0	0	1	n.d.	n.d.
XXIV	29	n.d.	n.d.	n.d.	n.d.	n.d.	n.d.	n.d.	n.d.	n.d.	n.d.	n.d.
XXV	30	Turkey	n.d.	n.d.	n.d.	n.d.	n.d.	n.d.	n.d.	n.d.	n.d.	n.d.
	31	Turkey	1	0	2	2	2	0	2	0	1	1
XXVI	32	Turkey	1	0	3	2	2	1	1	2	2	1
XXVII	33	UK	2	1	2	1	3	1	2	0	n.d.	1

IUGR = intrauterine growth retardation; n.d. = not determined; 0 = not present; 1 = mild; 2 = moderate; 3 = severe; neurodevelopmental features (psychomotor retardation, corpus callosum dysgenesis, athetoid movements, cataracts/corneal clouding) were given a double weight in the scoring.

site mutation, respectively. Evaluation by MutationTaster, PolyPhen2 and comparison with six vertebrate PYCR1 orthologs revealed that all residues affected by missense mutations are highly conserved and the changes were predicted to be pathogenic (Supplementary Fig. 3) [22]. Furthermore, we investigated whether these variants are present in the 1000 Genomes Project or the Exome Variant Server (EVS) data set. Interestingly, in the EVS data we found some of the known *PYCR1* mutations and other changes with high pathogenic potential with low frequency. On this basis, we estimate a frequency of 2×10^{-3} for pathogenic *PYCR1* mutations in the general population resulting in a frequency of homo- or compound heterozygous carriers of around 4×10^{-6}.

3.3. Spectrum and distribution of PYCR1 mutations and genotype–phenotype correlation

Analysis of the *PYCR1* mutation spectrum described so far revealed an accumulation of mutations in exons 4, 5, and 6 [18,24–36]. Except the p.Gly4Val, p.Gly4Asp and p.Ile30Lys mutations, which are in exons 1 and 2, respectively, 84% of the missense mutations observed resided in exons 4 to 6 (Fig. 3A). Also the mutations p.Gly4fs*50, c.138 + 1G>A, c.138 + 2T>C, and p.Gln10* were found in or adjacent to exons 1 and 2 (Fig. 3A). In order to gain insight into the structural and functional consequences of the missense mutations we mapped all known PYCR1 mutations to the 3D structure of the protein (Fig. 3B, Supplementary Fig. 2). Ten of the 16 amino acids affected by missense mutations were found to protrude to the surface of the protein. Probably functionally most relevant are the four residues (Arg119, Arg251, Arg266, Val258) that form part of the lateral surface of the PYCR1 monomer. These residues could make contact to the neighbouring PYCR1 homodimer and be involved in homodecamer formation [21]. In line with a role of Arg251 in homodimer interaction via hydrogen bonds predicted by the 3D structure the p.Arg251His mutation was shown to only mildly affect stability of the monomer [18]. On the other hand, the p.Arg119Gly mutation severely destabilized the protein [18]. No protein expression data was available for the p.Val258Met variant, which seems very likely to also influence homodecamer formation. Since Ala241 and Gly192 lie in a part of the protein intercalating with another monomer the p.Ala241Asp and p.Gly192Val mutations are likely to entail defective homodimer formation. Ala179, Gly248, Ala257, and Ala260 point to the inner surface of the ring-like PYCR1 homodecamer, which explains why the quite drastic change p.Gly248Glu only mildly reduced expression of the monomer [26]. The p.Ala260Pro mutation is likely to disrupt the long terminal alpha helix α13 (Supplementary Fig. 2).

Our collaborative network has accumulated the largest cohort of *PYCR1*-related ARCL affected individuals consisting of 68 patients from 49 families, which had partially been described previously [18,31]. Calculating the frequencies of different mutation types in all patients described so far we found that missense alterations (47%) are most frequent followed by splice site mutations (38%). The combination of splice site and missense mutation is present in 9% of all cases whereas nonsense or frameshift alterations are underrepresented (5%) (Fig. 4A).

Phenotypic findings												
HPO terms		HP:0000270	HP:0000252	HP:0001999	HP:0000592	HP:0000487	HP:0001274	HP:0006829	HP:0001263	HP:0002305	HP:0007957	
Family no.	Patient no.	Late fontanel closure	Microcephaly	Dysmorphic features	Blue sclerae	Strabismus	Corpus callosum dysgenesis	Hypotonia	Psychomotor retardation	Athetoid movements	Cataract/ corneal clouding	Clinical score
I	1	1	0	1	1	0	0	1	1	0	0	0.9
II	2	0	1	1	0	0	n.d.	1	1	0	0	0.6
	3	n.d.	0	1	0	0	n.d.	n.d.	1	0	0	0.5
III	4	1	1	1	0	1	n.d.	1	2	n.d.	0	0.9
	5	1	1	1	0	2	n.d.	1	2	n.d.	0	1.1
IV	6	0	0	1	0	0	0	0	0	0	0	0.5
V	7	1	0	1	0	1	n.d.	1	2	1	0	0.7
VI	8	n.d.	1	1	0	1	1	1	1	1	0	0.9
VII	9	1	1	1	1	1	0	0	2	0	0	1.1
VIII	10	n.d.	1	1	1	1	0	1	1	0	0	0.7
IX	11	n.d.	n.d.	n.d.	n.d.	n.d.	n.d.	n.d.	n.d.	n.d.	n.d.	1.3
X	12	n.d.	1	2	2	0	1	3	3	0	1	1.8
XI	13	n.d.	1	1	0	0	0	1	1	1	1	0.8
XII	14	n.d.	1	3	0	0	n.d.	1	3	1	n.d.	1.7
	15	n.d.	n.d.	2	0	n.d.	n.d.	1	3	1	n.d.	1.9
	16	n.d.	n.d.	2	0	n.d.	n.d.	1	3	1	n.d.	2
XIII	17	n.d.	2	2	0	0	n.d.	3	1	0	0	1.6
XIV	18	0	0	1	0	0	0	1	1	0	0	0.7
XV	19	n.d.	2	1	0	0	n.d.	1	1	0	0	1.2
XVI	20	1	2	2	2	1	n.d.	3	3	0	0	1.7
XVII	21	1	0	2	2	0	0	0	0	0	0	0.8
XVIII	22	2	0	1	1	0	n.d.	1	1	0	0	1.1
XIX	23	2	1	2	1	0	n.d.	1	1	0	0	1.1
	24	n.d.	n.d.	n.d.	n.d.	n.d.	n.d.	n.d.	1	n.d.	n.d.	1.3
XX	25	2	1	2	0	2	n.d.	2	n.d.	0	0	1.2
XXI	26	1	1	1	1	1	1	1	1	1	1	1.1
XXII	27	1	1	2	0	0	n.d.	1	1	0	0	0.6
XXIII	28	0	1	0	0	1	n.d.	1	3	1	0	1.1
XXIV	29	n.d.	n.d.	n.d.	2	2	n.d.	0	n.d.	1	2	1
XXV	30	n.d.	n.d.	1	1	n.d.	n.d.	1	1	n.d.	n.d.	1
	31	1	1	1	1	0	0	2	2	0	0	1.7
XXVI	32	1	0	1	1	1	0	0	2	0	0	1.2
XXVII	33	0	1	1	n.d.	0	1	2	n.d.	0	0	0.4

An overall clinical score was calculated on the basis of the severity or absence of up to 20 clinical features. The average score for all patients from our cohort was around 1 with a range between 0.4 and 1.9, indicating that each feature was on average mildly expressed in all individuals. Comparing the overall scores associated with the different mutation types no significant differences were seen (data not shown). Psychomotor retardation was present in all except of three affected individuals. Although these three individuals also had lower overall clinical scores, they had the typical outward appearance. Interestingly, both cases carrying the homozygous c.138 + 1G>A mutations were not intellectually disabled indicating that this splice site mutation has a mild effect. Low clinical scores and mild intellectual disability were associated with the most N-terminal mutations p.Gly4Val and p.Gly4Asp. In summary, there was a significant association of lower clinical scores and absent or only mild intellectual disability with mutations in exons 1 and 2 when compared to mutations in exons 4, 5, and 6 (Fig. 4B).

4. Discussion

Common clinical features of *PYCR1*-related ARCL include wrinkled and/or sagging skin, a typical facial dysmorphism, hyperlaxity of joints, growth retardation, hypotonia, and psychomotor developmental delay [18,24,31]. The difficulties of diagnosing the disorder on clinical grounds are mirrored by the diverse initial clinical diagnoses made in our patient group ranging from other cutis laxa syndromes to other progeroid disorders like Hallermann–Streiff syndrome or neonatal progeria. In mild cases, especially with normal psychomotor development, one might misdiagnose patients with *PYCR1* mutations as having gerodermia osteodysplastica [30,35]. More severe cases with significant retardation, epilepsy and pachygyria can be very similar to *ATP6V0A2*-related ARCL2A [12,17]. As already evident in the description by Annemarie Sommer of a case, in which we later found a PYCR1 mutation, progeroid features and growth delay usually get milder when the children grow up [18,37]. The frequency of "common" *PYCR1* mutation-related features in our patient group is comparable to that of previously reported cases. However, it should be noted that there is a discrepancy between the reported frequencies of hypotonia, osteopenia, finger contractures, and late fontanel closure. Interestingly, corneal clouding and cataracts have been suggested to be typical for *PYCR1* and *ALDH18A1* mutations [31]. But this was not confirmed in our study since only four patients suffered from these specific eye problems.

The type of neurologic involvement was highly variable and mostly not discriminative. Epilepsy, which has been up to now mostly observed in ARCL2A patients, occurred in three of our patients [38]. Athetoid movements, described as characteristic for *PYCR1* mutations were only present in nine patients, while a corpus callosum agenesis was present in one third of the patients in which a MRI was performed, suggesting that these signs support the diagnosis of *PYCR1*-related cutis laxa but the absence of corpus callosum abnormalities or extrapyramidal symptoms does not rule out the diagnosis. In conclusion, IUGR, hypotonia,

and psychomotor retardation together with the typical facial gestalt should allow successful differential diagnosis. More unique features, such as finger contractures, cataract, corneal clouding, agenesis of the corpus callosum or athetoid movements can serve as sufficient features making the diagnosis highly likely. However, it should be noted that due to the close clinical overlap there are no clinical features that allow distinguishing *ALDH18A1*- from *PYCR1*-related ARCL [31]. As a general rule *ALDH18A1*-related ARCL is more severe, especially the intellectual disability.

PYCR1 mutations are found in approximately 25% of ARCL2 cases and are, together with *ATP6V0A2* mutations, the most common cause of this disease spectrum [9]. In addition to the 37 patients we described previously we here present 33 individuals with *PYCR1*-related ARCL with seven novel mutations [18,31]. Including these newly identified alterations 30 different mutations in *PYCR1* have been reported. The majority are missense mutations, followed by splice site mutations, combinations of splice site and missense mutations, and nonsense or frameshift mutations. No significant correlation between mutation type and disease expression was detected. We previously described that all tested mutations result in PYCR1 protein degradation up to a total loss of the protein [18]. Given that the disease mechanism is therefore clearly a loss of function it might be surprising that so far only one nonsense mutation (p.Gln10*) has been identified. However, a similar underrepresentation of nonsense mutations has been reported in other metabolic disorders (e.g. phenylketonuria) [39]. The two siblings harbouring the p.Gln10* mutation as well as the two non-related patients with this mutation that have been described recently are of Brazilian origin [33]. It cannot be excluded that these families are related or at least come from the same region.

The majority of the missense mutations reside within exons 4 to 6, which encode the most highly conserved parts of the PYCR1 protein containing many residues involved in enzymatic function [21]. None of the mutations found in *PYCR1*-related ARCL precisely affect amino acids involved in enzymatic function, but often neighbouring residues. In one patient, the alteration p.Gly297Arg encoded by the alternative exon 8 was identified besides the known missense mutation p.Gly248Glu [26]. The C-terminus encoded by this alternative transcript is evolutionarily not conserved and we here show very low expression levels suggesting that this splice variant and mutations in it are of low clinical relevance.

Mutations affecting residues localized in the hydrophobic protein core are more likely to entail an overall folding problem leading to degradation. In contrast, changes in residues that lie at the protein surface can influence protein–protein interaction. It was shown that PYCR1 forms a homodimer which assembles into a ring-shaped homodecamer, which is finally biologically active [21]. We found that four mutated residues lie at the lateral surface of the PYCR1 monomer, which potentially gets in contact with the neighbouring homodimer. The p.Arg266Gln mutation is exceptional since it also strongly affects splicing which very likely impairs protein expression [24]. PYCR1 bearing the p.Arg119Gly mutation was severely destabilized indicating misfolding [18]. In contrast, previous results suggest that mutating Arg251, which forms a prominent protrusion on the protein surface and is known to stabilize homodimer formation though H bonding, only has a minor effect of

Table 2
Additional clinical findings, diagnoses and mutations.

				Mutations				
Family no.	Patient no.	Additional clinical findings	Initial diagnosis	Status	cDNA	Consequence	Exon	Literature mutation
I	1	Macular opacities	GO	hom	c.11G>A	p.Gly4Asp	1	Novel
II	2	–	CL	hom	c.11G>T	p.Gly4Val	1	Novel
	3	–	GO	hom	c.11G>T	p.Gly4Val		
III	4	Early death	ARCL2B	hom	c.28C>T	p.Q10*	1	[33]
	5	Early death	ARCL2B	hom	c.28C>T	p.Q10*		
IV	6	–	n.d.	hom	c.138 + 1G>A	Splicing	2	[18]
V	7	–	HS	het	c.138 + 2T>C	Splicing	2	Novel
				het	c.722C>T	p.Ala241Val	6	[33]
VI	8	–	DBS	hom	c.355C>T	p.Arg119Cys	4	[36]
VII	9	Tourette syndrome, ADHD	GO	hom	c.355C>G	p.Arg119Gly	4	[18]
VIII	10	Epilepsy	WSS	hom	c.535G>A	p.Ala179Thr	4	[18,35]
IX	11	–	n.d.	hom	c.535G>A	p.Ala179Thr	4	[18,35]
X	12	Glaucoma, hydroureteronephrosis, clubfoot, platybasia	DBS	het	c.349G>T	p.Val117Phe	4	Novel
				het	c.540 + 1G>A	Splicing	4	[18,30,31]
XI	13	–	DBS	hom	c.540 + 1G>A	Splicing	4	[18,30,31]
XII	14	–	n.d.	hom	c.540 + 1G>A	Splicing	4	[18,30,31]
	15	–	n.d.	hom	c.540 + 1G>A	Splicing		
	16	–	n.d.	hom	c.540 + 1G>A	Splicing		
XIII	17	Late dentition, pectus excavatum	n.d.	hom	c.540 + 1G>A	Splicing	4	[18,30,31]
XIV	18	Pes planus, ADHD, joint pain, pale optic discs	GO	hom	c.540 + 1G>A	Splicing	4	[18,30,31]
XV	19	–	n.d.	hom	c.540 + 1G>A	Splicing	4	[18,30,31]
XVI	20	Abnormal fat pads, syndactyly	Progeria	hom	c.575G>T	p.Gly192Val	5	Novel
XVII	21	Sparse hair	DBS	hom	c.616G>A	p.Gly206Arg	5	[18,25]
XVIII	22	–	DBS	hom	c.575G>T	p.Gly192Val	5	Novel
XIX	23	Abnormal fat pads	n.d.	hom	c.616G>A	p.Gly206Arg	5	[18,25]
	24	–	n.d.	hom	c.616G>A	p.Gly206Arg		
XX	25	Epilepsy	ARCL2B	hom	c.797 + 2-797 + 5_del	Splicing	6	[18]
XXI	26	Epilepsy	DBS	hom	c.772G>A	p.Val258Met	6	[34]
XXIII	27	–	ACL2	het	c.743G>A	p.Gly248Glu	6	[26]
				het	c.797G>A	Splicing	6	[18,24]
XXIII	28	–	Progeria	het	c.752G>A	p.Arg251His	6	[18]
				het	c.797 + 2-797 + 5del	Splicing	6	[18]
XXIV	29	–	DBS	hom	c.752G>A	p.Arg251His	6	[18]
XXV	30	–	DBS	hom	c.722C>A	p.Ala241Asp	6	Novel
	31	Sparse hair	CL	hom	c.722C>A	p.Ala241Asp	6	Novel
XXVI	32	Hydronephrosis	GO	hom	c.797 + 2-797 + 5_del	Splicing	6	[18]
XXVII	33	Absent cingulate gyrus, pectus carniatum, equinovarus feet	n.d.	het	c.778G>C	p.Ala260Pro	6	Novel
				het	c.797G >A	Splicing	6	[18,24]

ADHD = attention deficit hyperactivity disorder; CL = cutis laxa; DBS = De Barsy syndrome; HS = Hallermann–Streiff syndrome; GO = gerodermia osteodysplastica.

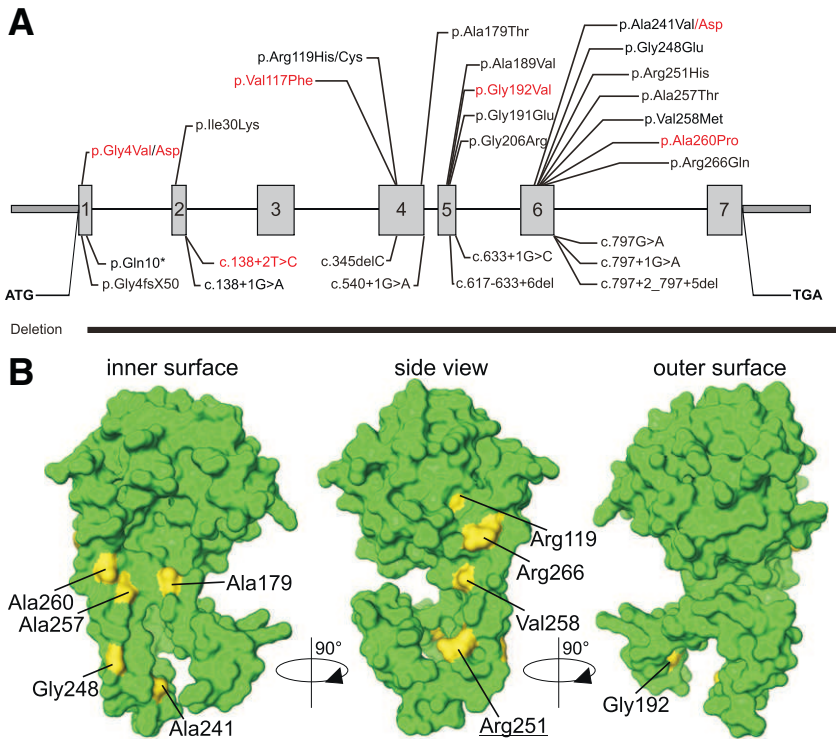

Fig. 3. Mutational spectrum of *PYCR1* and surface localization of residues affected by missense mutations. (A) A schematic overview of all known *PCYR1* mutations. On top of the exon overview all missense whereas below all other types of mutations are shown. Mutations described previously are indicated in black. Novel mutations identified in the present study are given in red. (B) 10 mutated amino acids affected by missense mutations (shown in yellow) are in contact with the surface of the PYCR1 protein. Four (Arg119, Arg251, Val258, Arg266) are at one side which makes contact to other PYCR1 homodimers in the ring-like homodecamer structure. Four affected residues (Ala179, Gly248, Ala257, Ala260) reside at the "back" of the molecule, which forms the inner surface of the ring-shaped homodecamer. Two mutated residues (Val192, Ala241) are at sites relevant for homodimer formation. No mutated residues are found at the outer surface where catalysis takes place and at the other lateral surface (Supplementary Fig. 2). Arg251 (underlined) is the only surface-localized residue with a direct role in stabilization of the inter-homodimer interaction.

protein stability [18,21]. Since patients bearing this mutation do not show a milder phenotype the functional loss might stem from defective PYCR1 multimerization. The effect of the mutations p.Gly192 and p.Ala241 on monomer stability and homodimer formation remains to be investigated.

The only three missense alterations not residing in exons 4 to 6 are p.Gly4Val, pGly4Asp and p.Ile30Lys. Interestingly, affected individuals with mutations in exons 1 and 2, including the "severe" p.Gln10* mutation, show low average clinical scores and three of these individuals do not show intellectual disability. The p.Gln10* mutation is highly likely to cause nonsense-mediated decay and thereby a total absence of the PYCR1 protein. A similar effect can be assumed for the c.138 + 1G>A mutation. For the mutations p.Gly4Val, p.Gly4Asp and p.Ile30Lys we propose a different pathomechanism. Given that PYCR1 is very likely an intra-mitochondrial protein, these mutations could affect mitochondrial import as well as sub-mitochondrial localization because of an altered targeting signal, which usually resides in the N-terminus. All these facts indicate that a reduction of the protein in mitochondria due to either complete loss of the mRNA or the gene product, or defective protein import is less deleterious for tissue function than the presence of an altered protein that cannot form a homodecamer and carry out its enzymatic function. This hypothesis is further underscored by the fact that also patients with a deletion of the entire *PYCR1* locus do not show intellectual disability [25]. This indicates that the absence of PYCR1 can be tolerated during development of the CNS. In contrast, PYCR1 seems more important for the development of skeletal, fat and connective tissues. In post-natal development, however, PYCR1 becomes less crucial explaining why the progeroid appearance and growth delay get milder with age. The investigation of PYCR1 function during different developmental stages and the consequences of mutations is subject of ongoing research.

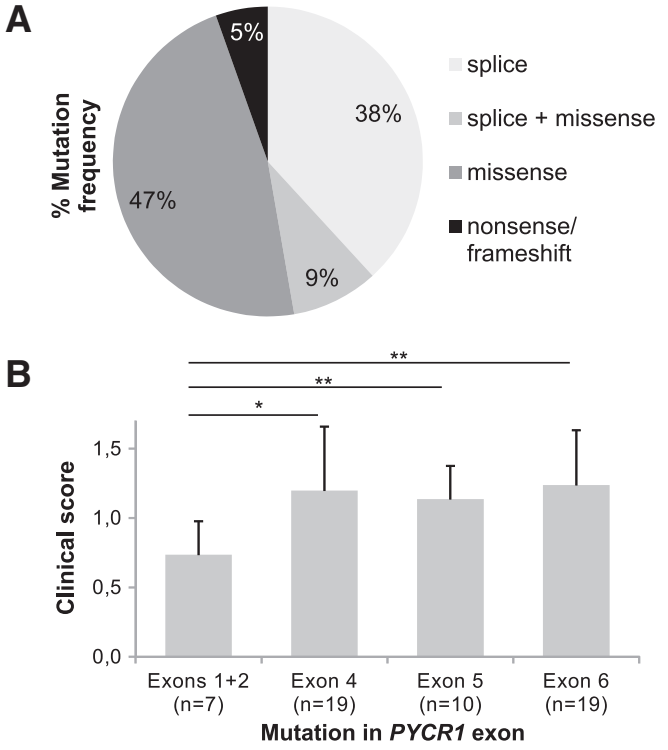

Fig. 4. Genotype–phenotype correlation. (A) Distribution of mutation types in all *PYCR1*-related ARCL individuals. (B) Clinical score in relation to the localization of the mutations within the *PYCR1* exons. A significantly lower clinical score is found for patients with mutations in exon 1 or 2. P-values were obtained using Students *t*-test (* = $P < 0.05$; ** = $P < 0.01$).

In conclusion, our current study presents the second largest group of patients with *PYCR1*-related ARCL and expands the clinical and genetic spectrum. Furthermore, by comparison with all patients reported so far we were able to determine the clinical features which are crucial for diagnosis of this clinically variable progeroid disorder. The analysis of the genotype–phenotype correlation might help to improve our understanding of the different functions of the PYCR1 protein during different phases of development.

Conflicts of interest statement

The authors declare no conflict of interest.

Web resources

Online Mendelian Inheritance in Man (OMIM) http://www.ncbi.nlm.gov/Omim/ (for ADCL and ARCL1 and ARCL2A, ARCL2B, DBS, MACS).

Acknowledgments

We are grateful to the patients and family members whose cooperation made this study possible. This study was funded by the Deutsche Forschungsgemeinschaft (KO 2891/1-1) to Uwe Kornak and the Radboud University Nijmegen Medical Center IGMD junior investigation grant.

Appendix A. Supplementary data

Supplementary data to this article can be found online at http://dx.doi.org/10.1016/j.ymgme.2013.08.009.

References

[1] B. Callewaert, M. Renard, V. Hucthagowder, B. Albrecht, I. Hausser, E. Blair, C. Dias, A. Albino, H. Wachi, F. Sato, R.P. Mecham, B. Loeys, P.J. Coucke, A. De Paepe, Z. Urban, New insights into the pathogenesis of autosomal-dominant cutis laxa with report of five ELN mutations, Hum. Mutat. 32 (2011) 445–455.
[2] J. Hoyer, C. Kraus, G. Hammersen, J.P. Geppert, A. Rauch, Lethal cutis laxa with contractural arachnodactyly, overgrowth and soft tissue bleeding due to a novel homozygous fibulin-4 gene mutation, Clin. Genet. 76 (2009) 276–281.
[3] V. Hucthagowder, N. Sausgruber, K.H. Kim, B. Angle, L.Y. Marmorstein, Z. Urban, Fibulin-4: a novel gene for an autosomal recessive cutis laxa syndrome, Am. J. Hum. Genet. 78 (2006) 1075–1080.
[4] B. Loeys, L. Van Maldergem, G. Mortier, P. Coucke, S. Gerniers, J.M. Naeyaert, A. De Paepe, Homozygosity for a missense mutation in fibulin-5 (FBLN5) results in a severe form of cutis laxa, Hum. Mol. Genet. 11 (2002) 2113–2118.
[5] B. Callewaert, C.T. Su, T. Van Damme, P. Vlummens, F. Malfait, O. Vanakker, B. Schulz, M. Mac Neal, E.C. Davis, J.G. Lee, A. Salhi, S. Unger, K. Heimdal, S. De Almeida, U. Kornak, H. Gaspar, J.L. Bresson, K. Prescott, M.E. Gosendi, S. Mansour, G.E. Pierard, S. Madan-Khetarpal, F.C. Sciurba, S. Symoens, P.J. Coucke, L. Van Maldergem, Z. Urban, A. De Paepe, Comprehensive clinical and molecular analysis of 12 families with type 1 recessive cutis laxa, Hum. Mutat. 34 (2013) 111–121.
[6] Z. Urban, V. Hucthagowder, N. Schurmann, V. Todorovic, L. Zilberberg, J. Choi, C. Sens, C.W. Brown, R.D. Clark, K.E. Holland, M. Marble, L.Y. Sakai, B. Dabovic, D.B. Rifkin, E.C. Davis, Mutations in LTBP4 cause a syndrome of impaired pulmonary, gastrointestinal, genitourinary, musculoskeletal, and dermal development, Am. J. Hum. Genet. 85 (2009) 593–605.
[7] H.C. Hennies, U. Kornak, H. Zhang, J. Egerer, X. Zhang, W. Seifert, J. Kuhnisch, B. Budde, M. Natebus, F. Brancati, W.R. Wilcox, D. Muller, P.B. Kaplan, A. Rajab, G. Zampino, V. Fodale, B. Dallapiccola, W. Newman, K. Metcalfe, J. Clayton-Smith, M. Tassabehji, B. Steinmann, F.A. Barr, P. Nurnberg, P. Wieacker, S. Mundlos, Gerodermia osteodysplastica is caused by mutations in SCYL1BP1, a Rab-6 interacting golgin, Nat. Genet. 40 (2008) 1410–1412.
[8] U. Kornak, E. Reynders, A. Dimopoulou, J. van Reeuwijk, B. Fischer, A. Rajab, B. Budde, P. Nurnberg, F. Foulquier, D. Lefeber, Z. Urban, S. Gruenewald, W. Annaert, H.G. Brunner, H. van Bokhoven, R. Wevers, E. Morava, G. Matthijs, L. Van Maldergem, S. Mundlos, Impaired glycosylation and cutis laxa caused by mutations in the vesicular H+-ATPase subunit ATP6V0A2, Nat. Genet. 40 (2008) 32–34.
[9] B. Fischer, A. Dimopoulou, J. Egerer, T. Gardeitchik, A. Kidd, D. Jost, H. Kayserili, Y. Alanay, I. Tantcheva-Poor, E. Mangold, C. Daumer-Haas, S. Phadke, R.I. Peirano, J. Heusel, C. Desphande, N. Gupta, A. Nanda, E. Felix, E. Berry-Kravis, M. Kabra, R.A. Wevers, L. van Maldergem, S. Mundlos, E. Morava, U. Kornak, Further characterization of ATP6V0A2-related autosomal recessive cutis laxa, Hum. Genet. 131 (11) (2012) 1761–1773.
[10] V. Hucthagowder, E. Morava, U. Kornak, D.J. Lefeber, B. Fischer, A. Dimopoulou, A. Aldinger, J. Choi, E.C. Davis, D.N. Abuelo, M. Adamowicz, J. Al-Aama, L. Basel-Vanagaite, B. Fernandez, M.T. Greally, G. Gillessen-Kaesbach, H. Kayserili, E. Lemyre, M. Tekin, S. Turkmen, B. Tuysuz, B. Yuksel-Konuk, S. Mundlos, L. Van Maldergem, R.A. Wevers, Z. Urban, Loss-of-function mutations in ATP6V0A2 impair vesicular trafficking, tropoelastin secretion and cell survival, Hum. Mol. Genet. 18 (2009) 2149–2165.
[11] E. Morava, R.A. Wevers, M.A. Willemsen, D. Lefeber, Cobblestone-like brain dysgenesis and altered glycosylation in congenital cutis laxa, Debre type, Neurology 73 (2009) 1164(author reply 1164–1165).
[12] L. Van Maldergem, M. Yuksel-Apak, H. Kayserili, E. Seemanova, S. Giurgea, L. Basel-Vanagaite, E. Leao-Teles, J. Vigneron, M. Foulon, M. Greally, J. Jaeken, S. Mundlos, W.B. Dobyns, Cobblestone-like brain dysgenesis and altered glycosylation in congenital cutis laxa, Debre type, Neurology 71 (2008) 1602–1608.
[13] B. Albrecht, A.P. de Brouwer, D.J. Lefeber, K. Cremer, I. Hausser, N. Rossen, S.B. Wortmann, R.A. Wevers, U. Kornak, E. Morava, MACS syndrome: a combined collagen and elastin disorder due to abnormal Golgi trafficking, Am. J. Med. Genet. A 152A (2010) 2916–2918.
[14] L. Basel-Vanagaite, O. Sarig, D. Hershkovitz, D. Fuchs-Telem, D. Rapaport, A. Gat, G. Isman, I. Shirazi, M. Shohat, C.D. Enk, E. Birk, J. Kohlhase, U. Matysiak-Scholze, I. Maya, C. Knopf, A. Peffekoven, H.C. Hennies, R. Bergman, M. Horowitz, A. Ishida-Yamamoto, E. Sprecher, RIN2 deficiency results in macrocephaly, alopecia, cutis laxa, and scoliosis: MACS syndrome, Am. J. Hum. Genet. 85 (2009) 254–263.
[15] A.M. de Barsy, E. Moens, L. Dierckx, Dwarfism, oligophrenia and degeneration of the elastic tissue in skin and cornea. A new syndrome? Helv. Paediatr. Acta 23 (1968) 305–313.
[16] J. Kunze, F. Majewski, P. Montgomery, A. Hockey, I. Karkut, T. Riebel, De Barsy syndrome—an autosomal recessive, progeroid syndrome, Eur. J. Pediatr. 144 (1985) 348–354.
[17] E. Leao-Teles, D. Quelhas, L. Vilarinho, J. Jaeken, De Barsy syndrome and ATP6V0A2-CDG, Eur. J. Hum. Genet. 18 (2010) 526(author reply 526).
[18] B. Reversade, N. Escande-Beillard, A. Dimopoulou, B. Fischer, S.C. Chng, Y. Li, M. Shboul, P.Y. Tham, H. Kayserili, L. Al-Gazali, M. Shahwan, F. Brancati, H. Lee, B.D. O'Connor, M. Schmidt-von Kegler, B. Merriman, S.F. Nelson, A. Masri, F. Alkazaleh, D. Guerra, P. Ferrari, A. Nanda, A. Rajab, D. Markie, M. Gray, J. Nelson, A. Grix, A. Sommer, R. Savarirayan, A.R. Janecke, E. Steichen, D. Sillence, I. Hausser, B. Budde, G. Nurnberg, P. Nurnberg, P. Seemann, D. Kunkel, G. Zambruno, B. Dallapiccola, M. Schuelke, S. Robertson, H. Hamamy, B. Wollnik, L. Van Maldergem, S. Mundlos, U. Kornak, Mutations in PYCR1 cause cutis laxa with progeroid features, Nat. Genet. 41 (2009) 1016–1021.
[19] L.S. Bicknell, J. Pitt, S. Aftimos, R. Ramadas, M.A. Maw, S.P. Robertson, A missense mutation in ALDH18A1, encoding Delta1-pyrroline-5-carboxylate synthase (P5CS), causes an autosomal recessive neurocutaneous syndrome, Eur. J. Hum. Genet. 16 (2008) 1176–1186.
[20] J.M. Phang, J. Pandhare, Y. Liu, The metabolism of proline as microenvironmental stress substrate, J. Nutr. 138 (2008) 2008S–2015S.
[21] Z. Meng, Z. Lou, Z. Liu, M. Li, X. Zhao, M. Bartlam, Z. Rao, Crystal structure of human pyrroline-5-carboxylate reductase, J. Mol. Biol. 359 (2006) 1364–1377.
[22] J.M. Schwarz, C. Rodelsperger, M. Schuelke, D. Seelow, MutationTaster evaluates disease-causing potential of sequence alterations, Nat. Methods 7 (2010) 575–576.
[23] P.N. Robinson, S. Kohler, S. Bauer, D. Seelow, D. Horn, S. Mundlos, The Human Phenotype Ontology: a tool for annotating and analyzing human hereditary disease, Am. J. Hum. Genet. 83 (2008) 610–615.
[24] D.L. Guernsey, H. Jiang, S.C. Evans, M. Ferguson, M. Matsuoka, M. Nightingale, A.L. Rideout, S. Provost, K. Bedard, A. Orr, M.P. Dube, M. Ludman, M.E. Samuels, Mutation in pyrroline-5-carboxylate reductase 1 gene in families with cutis laxa type 2, Am. J. Hum. Genet. 85 (2009) 120–129.
[25] R. Kretz, B. Bozorgmehr, M.H. Kariminejad, M. Rohrbach, I. Hausser, A. Baumer, M. Baumgartner, C. Giunta, A. Kariminejad, J. Haberle, Defect in proline synthesis: pyrroline-5-carboxylate reductase 1 deficiency leads to a complex clinical phenotype with collagen and elastin abnormalities, J. Inherit. Metab. Dis. 34 (2011) 731–739.
[26] D.S. Lin, J.H. Chang, H.L. Liu, C.H. Wei, C.Y. Yeung, C.S. Ho, C.H. Shu, M.F. Chiang, C.K. Chuang, Y.W. Huang, T.Y. Wu, Y.R. Jian, Z.D. Huang, S.P. Lin, Compound heterozygous mutations in PYCR1 further expand the phenotypic spectrum of De Barsy syndrome, Am. J. Med. Genet. A 155A (2011) 3095–3099.
[27] D.S. Lin, C.Y. Yeung, H.L. Liu, C.S. Ho, C.H. Shu, C.K. Chuang, Y.W. Huang, T.Y. Wu, Z.D. Huang, Y.R. Jian, S.P. Lin, A novel mutation in PYCR1 causes an autosomal recessive cutis laxa with premature aging features in a family, Am. J. Med. Genet. A 155A (2011) 1285–1289.
[28] D. Martinelli, J. Haberle, V. Rubio, C. Giunta, I. Hausser, R. Carrozzo, N. Gougeard, C. Marco-Marin, B.M. Goffredo, M.C. Meschini, E. Bevivino, S. Boenzi, G.S. Colafati, F. Brancati, M.R. Baumgartner, C. Dionisi-Vici, Understanding pyrroline-5-carboxylate synthetase deficiency: clinical, molecular, functional, and expression studies, structure-based analysis, and novel therapy with arginine, J. Inherit. Metab. Dis. 35 (5) (2012) 761–776.
[29] D.L. Skidmore, D. Chitayat, T. Morgan, A. Hinek, B. Fischer, A. Dimopoulou, G. Somers, W. Halliday, S. Blaser, Y. Diambomba, E.G. Lemire, U. Kornak, S.P. Robertson, Further expansion of the phenotypic spectrum associated with mutations in ALDH18A1, encoding Delta(1)-pyrroline-5-carboxylate synthase (P5CS), Am. J. Med. Genet. A 155A (2011) 1848–1856.
[30] Y. Yildirim, A. Tolun, B. Tuysuz, The phenotype caused by PYCR1 mutations corresponds to geroderma osteodysplasticum rather than autosomal recessive cutis laxa type 2, Am. J. Med. Genet. A 155A (2011) 134–140.
[31] S. Zampatti, M. Castori, B. Fischer, P. Ferrari, L. Garavelli, C. Dionisi-Vici, E. Agolini, A. Wischmeijer, E. Morava, G. Novelli, J. Haberle, U. Kornak, F. Brancati, De Barsy Syndrome: a genetically heterogeneous autosomal recessive cutis laxa syndrome related to P5CS and PYCR1 dysfunction, Am. J. Med. Genet. A 158A (2012) 927–931.

[32] M. Al-Owain, S. Alanazi, O. Khalifa, A. Al-Hemidan, L. Al-Ebdi, B. Al-Saud, F.S. Alkuraya, A case of de Barsy syndrome with a severe eye phenotype, Am. J. Med. Genet. A 158A (2012) 2364–2366.
[33] D.Z. Scherrer, M.B. Baptista, A.H. Matos, C.V. Maurer-Morelli, C.E. Steiner, Mutations in PYCR1 gene in three families with autosomal recessive cutis laxa, type 2, Eur. J. Med. Genet. 56 (6) (2013) 336–339.
[34] T. Gardeitchik, M. Mohamed, B. Fischer, M. Lammens, D. Lefeber, B. Lace, M. Parker, K.-J. Kim, B.C. Lim, J. Häberle, L. Garavelli, S. Jagadeesh, A. Kariminejad, D. Guerra, M. Leao, R. Keski-Filppula, L. Nijtmans, B. van der Heuvel, U. Kornak, E. Morava, Clinical and biochemical features guiding the diagnostics in neurometabolic cutis laxa, Eur. J. Hum. Genet. (2013)(in press).
[35] D. Kouwenberg, T. Gardeitchik, R.A. Wevers, J. Haberle, E. Morava, Recognizable phenotype with common occurrence of microcephaly, psychomotor retardation, but no spontaneous bone fractures in autosomal recessive cutis laxa type IIB due to PYCR1 mutations, Am. J. Med. Genet. A 155A (2011) 2331–2332(author reply 2333–2334).
[36] N. Nouri, O. Aryani, B. Kamalidehghan, M. Houshmand, Cutis laxa type II with mutation in the pyrroline-5-carboxylate reductase 1 gene, Pediatr. Dermatol. (2013).
[37] A. Sommer, Photo essay—geroderma, Am. J. Med. Genet. C Semin. Med. Genet. 145C (2007) 291–292.
[38] E. Morava, M. Guillard, D.J. Lefeber, R.A. Wevers, Autosomal recessive cutis laxa syndrome revisited, Eur. J. Hum. Genet. 17 (2009) 1099–1110.
[39] S.W. Gersting, K.F. Kemter, M. Staudigl, D.D. Messing, M.K. Danecka, F.B. Lagler, C.P. Sommerhoff, A.A. Roscher, A.C. Muntau, Loss of function in phenylketonuria is caused by impaired molecular motions and conformational instability, Am. J. Hum. Genet. 83 (2008) 5–17.